August 27-31, 2023
FLORENCE - ITALY
ICWE 16
16th International Conference on Wind Engineering

Wind tunnel experiment and CFD simulation of sand surface deformation around a cubic obstacle

Yoshihide Tominaga [1]

[1]*Wind and Fluid Engineering Research Center, Niigata Institute of Technology, Kashiwazaki, Japan, tominaga@abe.niit.ac.jp*

SUMMARY:
A wind tunnel experiment on sand surface deformation around a cubic obstacle was performed to elucidate the underlying fundamental phenomena and obtain validation data for a computational fluid dynamics (CFD) analysis. Erosion and deposition patterns on the wind-blown sand surface were measured using real sand grains. Considerable wind erosion was observed near the windward corners of the cube, in contrast to the low deposition in other areas. A primary CFD analysis of the wind erosion was conducted to reproduce the results of the experiment. A dynamic mesh technique was introduced to reproduce the time-dependent deformation of the sand surface. The results confirmed that the various shapes of the large erosion regions near the upwind corners of the cube were accurately reproduced by CFD analysis, even when relatively simple modeling of sand transport was performed. However, the erosion area in the prediction results was horizontally wider than that in the experimental results. These differences were mainly due to ignoring the relation between the horizontal movement of sand particles and the angle of repose in the CFD simulation.

Keywords: sand erosion, cubic obstacle, wind tunnel experiment, CFD

1. INTRODUCTION

Aeolian sand transport is accompanied by erosion and deposition processes, and each transport process can result in significant environmental damage. Erosion often results in land degradation, abrasion, deflation, evaporation, desertification, harmful airborne dust, and crop damage. Characteristic erosion occurs especially around obstacles because of the complex interaction between disturbed wind flows and sand movement behaviors. Therefore, accurate prediction of these phenomena is crucial in various engineering applications.

Sand movement around flow obstacles has been studied in relation to sand saltation around roughness elements. Iversen et al. (1990) pointed out that “the presence of non-erodible roughness elements in the midst of a bed of saltatable particles creates two primary effects on the saltation process, i.e., (1) it increases the value of threshold shear stress and (2) it decreases the mass transport for a given value of shear stress.” Furthermore, as reported by several researchers (Iversen et al., 1990; Sutton and Mckenna Neuman, 2008; Mckenna Neuman and Bédard, 2015), observations of the saltation patterns surrounding single roughness elements showed that the stress on the surface of the erodible bed was far from uniform. Therefore, “a complex pattern of

net surface erosion and deposition exists surrounding an object, whether or not the surface shear stress on the bed upwind is above a general threshold" (Iversen et al., 1990). By providing a quantitative prediction method for blown sand and sand erosion/deposition resulting from the complicated wind flow around obstacles, more effective countermeasures can be developed.

In this study, a wind tunnel experiment was conducted to illustrate the phenomena of the deformation of the sand surface around a surface-mounted cubic obstacle and obtain data for the validation of a computational fluid dynamics (CFD) analysis. The experiment was performed in an atmospheric boundary layer wind tunnel. A CFD analysis of the wind erosion was then conducted to reproduce the results of the experiment. The basic performance of the CFD simulations was validated by comparing the simulation results with those of the experiment.

2. WIND TUNNEL EXPERIMENT ON SAND EROSION

The details of the experiment have been reported by Tominaga et al. (2018). The experimental setup is shown in Figure 1. The experiment was conducted using the atmospheric boundary layer wind tunnel of dimension 1.8 × 1.8 × 13.0 m at the Niigata Institute of Technology. The floor of the measurement section was uniformly covered by a layer of sand 30 mm deep over a length extending to 15H (H: height of the cube = 200 mm) from the windward edge. The height difference between the floor of the wind tunnel and the sand surface was compensated for by a tapered surface. The cube model was placed 5H from the windward edge of the sand surface.

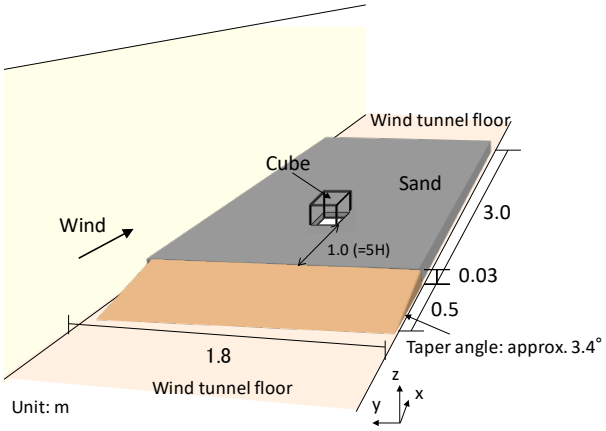

Figure 1. Setup of wind tunnel experiment.

The accumulated sand depth around the cube was measured at 67 locations. The sand depth was measured visually by moving a ruler using a traverse device with a precision of 1 mm. The experimental wind velocity was set such that the wind velocity at the boundary layer height (1000 mm from the floor surface = 5H) U_R without the cube was 12.0 m/s (the velocity at the cube height U_H was 7.3 m/s accordingly). This value was chosen based on a preliminary experiment in which the sand surface deformation stabilized after approximately 10 min at this wind velocity. Finally, the experiment was repeated four times by blowing the wind for 5, 10, 15, and 20 min, which are expressed as 10,950, 21,900, 38,850, and 43,800, respectively, in dimensionless time t^* (= $U_H t/H$).

3. COMPUTATIONAL SETUP

3.1. Computational Methods and Conditions

The CFD simulations were performed using the actual scale of the wind tunnel experiment. ANSYS Fluent 19.2 was used to solve the governing equations using the finite-volume approach for solving the Reynolds-averaged Navier–Stokes (RANS) equations. The realizable k–ε equation was used for the turbulence model. The computational conditions followed the guidelines proposed by the Architectural Institute of Japan (Tominaga et al., 2008). An unstructured mesh with 893,609 tetrahedral and prism cells was used.

3.2. Modeling of Sand Transport

In this study, only saltation was modeled. The following equation, proposed by Bagnold (1941), was used as the model for the horizontal sand saltation flux, q_{salt} [kg/m·s]:

$$q_{salt} = C\sqrt{\frac{d^p}{D}}\frac{\rho}{g}u_*(u_*^2 - u_{*t}^2) \quad (1)$$

Here, d^p is the grain diameter (0.5 mm in the present work), D is a reference sand grain diameter (0.25 mm, regardless of the value of d^p), ρ is the density of the fluid [kg/m^3], u_* is the friction velocity [m/s], u_{*t} is the threshold friction velocity [m/s], g is the gravitational acceleration [m/s^2], and C is a constant (the value of 1.8, which was proposed in Bagnold (1941), was used). To compute the vertical displacement of each cell, in each time step, the vertical flux Q_{salt} [kg/m^2·s] must be obtained. The vertical flux is assumed to be a fraction of the horizontal flux q_{salt} (Gillete and Passi, 1988). The mean jump length of saltation L_{salt} (m) is introduced as the length scale that relates the two fluxes (Andreotti et al., 2002; Almeida et al., 2008).

$$L_{salt} = 1091.5\left(\frac{\nu^2}{g}\right)^{\frac{1}{3}}(u_* - u_{*t})/\sqrt{gd^p} \quad (2)$$

where ν is the kinematic viscosity of the fluid [m^2/s]. The vertical flux caused by saltation is then calculated by

$$Q_{salt} = \frac{q_{salt}}{L_{salt}} \quad (3)$$

Once Q_{salt} is calculated for each cell on the sand surface, the vertical change per unit time in each cell Δh_i is expressed by

$$\Delta h_i = \frac{Q_{salt}\Delta t}{\rho^p} \quad (4)$$

where ρ^p is the bulk density of the sand grain [kg/m^3].

Based on the amount of change in each surface cell, transient calculations were performed using the dynamic mesh feature in Fluent by changing the CFD mesh at each time step. In this model, because Q_{salt} was always positive, only erosion occurred.

4. RESULTS AND DISCUSSION

Figure 2 shows a comparison of the results of the wind tunnel experiment and CFD simulations for the distribution of the sand accumulation ratio at t^* = 10,950 (5 min). From the CFD results, the distribution of the sand accumulation showed that erosion occurred at the windward corners of the cube, spreading out downwind in an elliptical shape. However, sand was deposited as a ridge in the center region in front of the obstacle. This result is in general agreement with the experimental results.

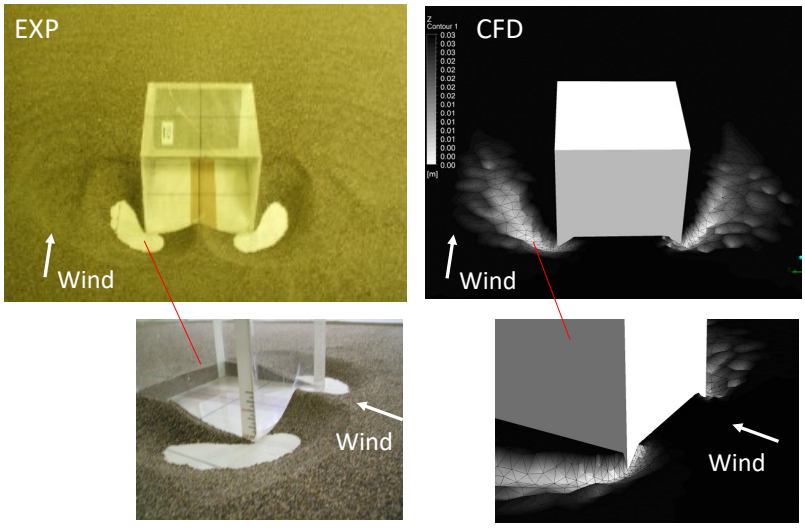

Figure 2. Distributions of sand accumulation ratio at t* = 10,950 for experiment and CFD simulation.

5. CONCLUSIONS

A CFD simulation of the erosion resulting from sand saltation was conducted based on data obtained in a wind tunnel experiment to illustrate the basic performance and applicability of the simulation method. The simulation reproduced the large erosion regions at the windward corners of the cube that were observed in the experiment, even with a relatively simple model. In future research, the sand transport model should be investigated further using the results of this study.

REFERENCES

Almeida, M. P., Parteli E. J. R., Andrade, J. S., and Herrmann, H. J., 2008. Giant saltation on Mars. Proceedings of the National Academy of Sciences 105(17), 6222–6226.

Andreotti, B., Claudin, P., and Douady, S., 2002. Selection of dune shapes and velocities Part 1: dynamics of sand, wind and barchans. The European Physical Journal B - Condensed Matter and Complex Systems 28, 321–339.

Bagnold, R. A., 1941. The Physics of Blown Sand and Desert Dunes, Mathuen, London.

Gillette, D. A., and Passi, R., 1988. Modeling dust emission caused by wind erosion. Journal of Geophysical Research: Atmospheres 93(D11), 14233–14242.

Iversen, J. D., Wang, W. P., Rasmussen, K. R., Mikkelsen, H. E., Hasiuk, J. F., and Leach, R. N., 1990. The effect of a roughness element on local saltation transport. Journal of Wind Engineering and Industrial Aerodynamics 36, 845–854.

McKenna Neuman, C., and Bédard, O., 2015. A wind tunnel study of flow structure adjustment on deformable sand beds containing a surface-mounted obstacle. Journal of Geophysical Research: Earth Surface 120, 1824–1840, doi:10.1002/2015JF003475.

Melbourne, W. H., 1980. Comparison of measurements on the CAARC standard tall building model in simulated model wind flows. Journal of Wind Engineering and Industrial Aerodynamics 6, 73–88.

Sutton, S. L. F., and McKenna Neuman, C., 2008. Sediment entrainment to the lee of roughness elements: Effects of vortical structures. Journal of Geophysical Research: Earth Surface 113, F02S09, doi:10.1029/2007JF000783.

Tominaga, Y., Okaze, T., and Mochida, A., 2018. Wind tunnel experiment and CFD analysis of sand erosion/deposition due to wind around an obstacle. Journal of Wind Engineering and Industrial Aerodynamics 182, 262–271.

Tominaga, Y., Mochida, A., Yoshie, R., Kataoka, H., Nozu, T., Yoshikawa, M., and Shirasawa, T., 2008. AIJ guidelines for practical applications of CFD to pedestrian wind environment around buildings. Journal of Wind Engineering and Industrial Aerodynamics 96(10–11), 1749–1761.